Phase Separation by Continuous Quenching: Similarities between Cooling Experiments in Polymer Blends and Reaction-Induced Phase Separation in Modified Thermosets

Ingo Alig, Maximilian Rüllmann, Marco Holst, Jianjun Xu*

Deutsches Kunststoff-Institut, Schloßgartenstraße 6, D-64289 Darmstadt, Germany

Summary: Small angle light scattering (SALS) has been applied to study the phase separation kinetics in a binary polymer mixture of poly(ethyl methyl siloxane) (PEMS) and poly(dimethyl siloxane) (PDMS). The phase separation was induced by cooling an initially homogeneous mixture with well defined cooling rates. The results have been compared to time resolved SALS and microscopy in the course of reaction-induced phase separation in mixtures of an epoxy resin and polysulfone (PSU).

For the critical PEMS/PDMS mixture with an upper critical point it was found in a continuous quenching experiment that the time evolution of the scattered light intensity $I(q,t)$ scales with the cooling rate. The similarity to the scaling behavior of $I(q,t)$ in isothermal experiments after fast quenches (scaled by the quench depth) is discussed. A secondary phase separation was found and has been explained by the competition between the growth of the two phase structure during cooling and the mutual diffusion without the assumption of gelation or vitrification.

For the epoxy/PSU mixture with 15% PSU, after the appearance of a bicontinuous structure a secondary phase separation was observed. Mixtures with higher PSU-contents formed epoxy-rich droplets in the PSU-rich matrix by nucleation and growth mechanism. The frustration of the structure growth can be explained by approaching vitrification of one or both phases.

The similarity between continuous cooling experiments in blends and the reaction-induced phase separation have been discussed in the generalized χN vs. composition phase diagram (N: degree of polymerization, χ: Flory-Huggins interaction parameter).

Keywords: continuous quenching, phase separation, polymer blends, thermosets

Introduction

The conventional experiment to investigate the phase separation kinetics in binary polymer mixtures is to transfer an initially homogeneous mixture by (almost) instantaneous changes of

 DOI: 10.1002/masy.200350821

temperature or pressure into the two phase region of the phase diagram and to detect the isothermal coarsening of the structure by time resolved microscopy or scattering experiments [1]. Due to the finite thermal conductivity it is practically impossible to realize an instantaneous transfer of a homogeneous mixture into the two phase region. An alternative experiment is to transfer a homogeneous mixture continuously into the two phase region. As schematically shown in the χN-phase diagram ($\chi(T, p)$: Flory-Huggins interaction parameter, N: degree of polymerization) in Scheme I a binary mixture can be continuously transferred from the one phase region into the two phase region by changing temperature, T, or pressure, p. This "χ-induced decomposition" can be realized by cooling (upper critical solution temperature) or heating (lower critical solution temperature) of the mixture. The cooling or heating rate becomes an additional parameter in this type of experiments. Alternatively, continuous pressure changes can be applied. Continuous quenching experiments are of practical importance for processing of polymer blends (e.g., mould injection).

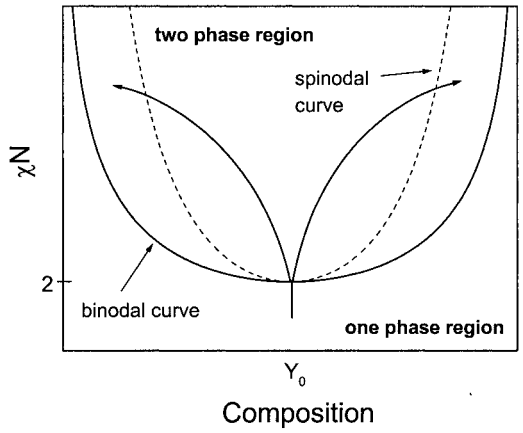

Scheme I. Continuous χ- and N-induced decomposition in the χN -phase diagram.

Two decades ago, Carmesin et al. [2] considered in a theoretical study the early stage of demixing of polymer blends during continuous quenching. More recently, Kukushkin and Slyonzov [3-5]] discussed in several theoretical papers the Oswald ripening under non-isothermal conditions. However, to our knowledge, no systematic experimental investigations of this type have been reported so far for polymer blends. Hashimoto et al. [6] and Hayashi et al. [7]

investigated the phase separation kinetics of polymer mixtures after a two step temperature change.

As obvious in Scheme I, a homogeneous mixture can also be transferred into the two phase region by increasing the degree of polymerization (reaction-induced or "*N*-induced" phase separation). A typical example is the reaction-induced phase separation of thermosets containing a chemically inert second component during isothermal curing experiments (see [8] and references therein).

It is the aim of this paper to discuss the similarities between continuous cooling experiments in polymer mixtures and the reaction-induced phase separation in quasi-binary thermoset blends. Therefore we applied time resolved small-angle light scattering (SALS) experiments and optical microscopy (OM) to mixtures of poly(ethyl methyl siloxane) and poly(dimethyl siloxane) while the mixtures were cooled with well defined cooling rates and to mixtures of an epoxy resin and polysulfone during isothermal curing.

Method

Recently we reported the details of a light scattering setup for investigation of phase separation kinetics in polymer mixtures after pressure jumps [9]. In this study the pressure cell was replaced by an electrically heated brass block, into which a sample holder was inserted. The sample thickness is 1 mm for the blend and 0.025 mm for the thermoset/thermoplastic mixtures. The accuracy of the temperature control of the sample was ± 5 mK for isothermal experiments and the cooling rates could be chosen between ± 10 mK/min and ± 0.3 K/min. The scattering vector q is given by $q = 4\pi n \sin(\theta/2)/\lambda_0$, where n is the refractive index, θ is the scattering angle, and λ_0 (= 632.8 nm) the wave length.

Samples

The polymer blend (System I) considered in this study is a binary mixture of poly(dimethyl siloxane) (PDMS) and poly(ethyl methyl siloxane) (PEMS), with molar masses of M_w = 18500 g/mol (M_w/M_n = 1.055) and M_w = 23927 g/mol (M_w/M_n = 1.049), respectively. The cloud point curve in Figure 1 (left part) shows an upper critical solution temperature. The spinodal (dashed) and the binodal curve (solid) are calculated using the Flory-Huggins theory.

In order to study the reaction-induced phase separation, blends of epoxy resin with polysulfone (PSU) have been prepared (for details see [10, 11]). The epoxy resin is diglycidyl ether of bisphenol-A (DGEBA, MY 790-1 from Ciba with M_n = 173.8 g/mol) cured with hexahydrophthalic anhydride (HHPA), using 2-ethyl-4-methylimidazole (EMI) as the catalyst. The mass ratio of DGEBA/HHPA/EMI was 120:100:2.4. PSU with M_n = 4900 g/mol and M_w = 11100 g/mol, was supplied by BASF with 99.9 % Cl-end group and 0.1 % OH-end group. The "phase diagram" in the coordinates of conversion versus volume fraction Φ_{PSU} of PSU is shown in Figure 1 (right part). The conversion was measured by differential scanning calorimetry and fitted by a modified Horie equation [10, 11]. The phase separation was investigated by OM, SALS and/or rheological measurements as described in [9, 11]. The gelation of the epoxy-rich phase ($\Phi_{PSU} < 0.15$) and the vitrification of the PSU-rich phase were determined from rheological experiments. The final conversion was estimated from calorimetric experiments. The vitrification curve, $T_g(\Phi_{PSU})$, was calculated from quasi-binary model using the Fox-equation and the DiBenedetto equation [11].

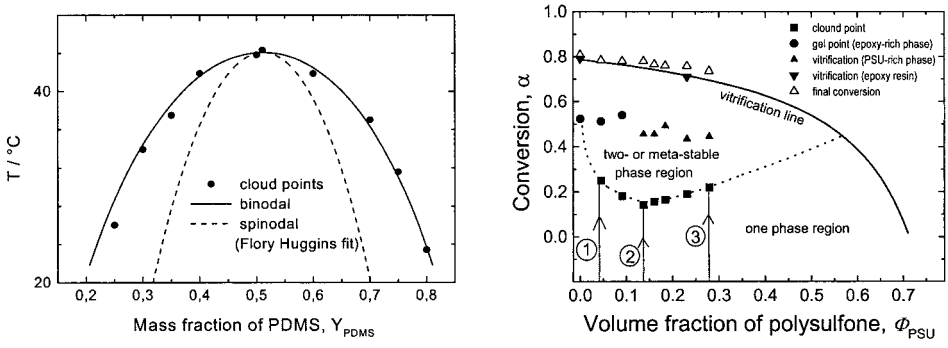

Figure 1. Phase diagram of the PDMS/PEMS mixture (left) and conversion versus composition diagram for the epoxy/PSU mixtures (right) cured at 80°C.

Continuous quenching of a binary blend

Figure 2 shows the time evolution of the scattered light intensity versus q for the critical mixture (Y_{PDMS} = 0.51) of PEMS/PDMS during a continuous cooling experiment (cooling rate: κ = 50 mK/min). After crossing the cloud point curve (t=0) a maximum in the scattering intensity (first

peak) appears in the experimental accessible q-range. The maximum scattering intensity of the main peak I_{m1} increases and the related scattering vector q_{m1} decrease with time. This feature is typical for coarsening of a two phase structure (spinodal decomposition). At later times a second shoulder or maximum becomes visible. The maximum scattering intensity of the second peak/shoulder I_{m2} also increases and the related scattering vector q_{m2} decreases with time, which is an indication for the development of a secondary structure inside the domains of the bicontinuous primary structure.

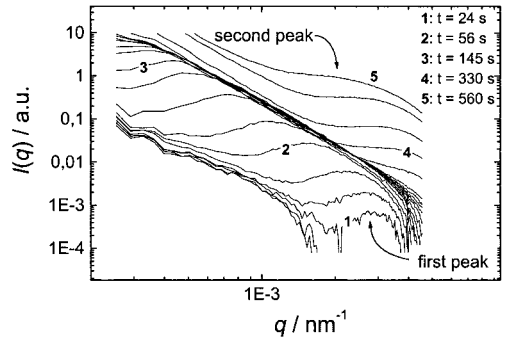

Figure 2. Time evolution of the scattering intensity during cooling of the critical PEMS/PDMS mixture ($Y_{PDMS} = 0.51$, cooling rate: $\kappa = 50$ mK/min).

The time evolutions of q_{m1} and q_{m2} are plotted in the left part of Figure 3 for three selected cooling rates κ. The corresponding values for I_{m1} and I_{m2} are shown in the inset. The time t is rescaled for both plots by the undercooling $\Delta T = \kappa \cdot t$. The values of $q_m(t)$ and $I_m(t)$ for different cooling rates can be shifted onto a master curve as shown in right part of Figure 3 for three selected cooling rates. This *cooling rate-scaling* is analogous to *quench depth-scaling* for instantaneous quenches and isothermal phase separation (see e.g. [1]). The reduced variables in Figure 3 are defined by: $q_{red} = q_m / q_{m,0}$ and $\Delta T_{red} = \Delta T / \Delta T_c = t_{red} = t / t_c$. $q_{m,0}$ is the q-vector at short times corresponding to a characteristic length l_c.

The inverse shift factors for the horizontal and vertical shifts are the characteristic undercooling ΔT_c (or the characteristic time t_c) and the characteristic scattering vector $q_{m,0} = q_m(0)$. In Figure 4 the values for ΔT_c (left part) and $q_{m,0}$ (right part) versus cooling rate κ are shown. The lines are fits with

power laws ($\Delta T_c(\kappa) = \Delta\hat{T} \cdot \kappa^{\vartheta}$ and $q_{m,0}(\kappa) = \hat{q} \cdot \kappa^{\zeta}$) to the data from the first peak for a set of experiments with five different cooling rates. The fitting values are $\Delta\hat{T} = 1.71\,\mathrm{K}^{0.71}\mathrm{s}^{0.29}$ and $\vartheta = 0.29$ for ΔT_c and $\hat{q} = 8.77 \cdot 10^{-3}\ \mathrm{nm}^{-1}\mathrm{s}^{0.18}\mathrm{K}^{-0.18}$ and $\zeta = 0.18$ for $q_{m,0}$. In [12,13] it is shown that the exponents $\vartheta = 0.29$ and $\zeta = 0.18$ are related to well known critical exponents.

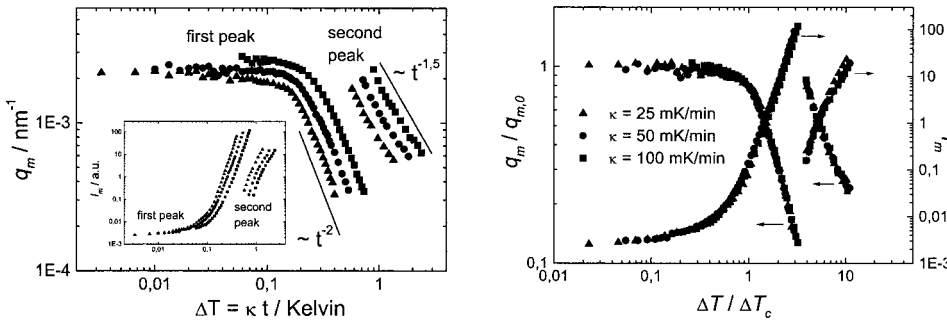

Figure 3. Evolution of scattering vectors (left part) for the first ($q_{m,1}$) and second peak ($q_{m,2}$) for the critical PEMS/PDMS mixture for different cooling rates κ. The time t is replaced by the undercooling: $\Delta T = \kappa\, t$. The corresponding intensities $I_{m,1}$ and $I_{m,2}$ are shown the inset. The right part shows the reduced plots for scattering vectors ($q_{m,1}$, $q_{m,2}$) and the intensities ($I_{m,1}$, $I_{m,2}$) versus the reduced undercooling, $\Delta T_{red} = \Delta T / \Delta T_c$.

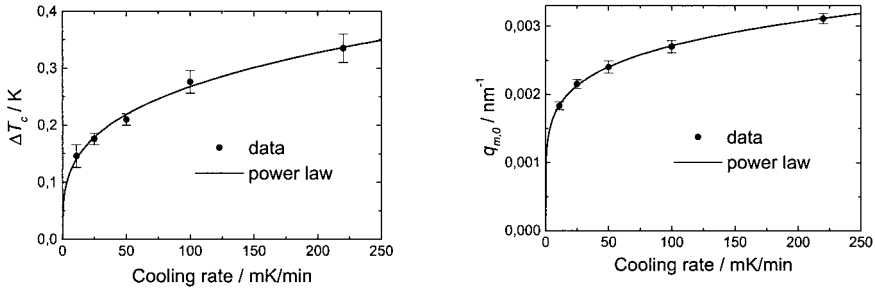

Figure 4. Scaling variables $q_{m,o}$ and ΔT_c (inverse shift factors from Figure 3) versus cooling rate κ for the critical PEMS/PDMS mixture.

As indicated in Figure 4, ΔT_c is the characteristic undercooling where both $q_{m,1}(\Delta T)$ and $I_{m,1}(\Delta T)$, show a crossover to a power law behavior. Based on the knowledge of structure growth in isothermal experiments, such a power law behavior in cooling experiments is expected for the late stage of demixing ($t > t_c$), by assuming a self-similar coarsening and thermodynamic equilibrium of the coexisting phases [12, 13]. Details of the expected power law behavior are discussed below.

As schematically shown in the phase diagram (Scheme II) the characteristic undercooling ΔT_c corresponds to the time t_c where for a given cooling rate κ the compositions of the two phases become identical to the corresponding binodal compositions. This follows from a thorough analysis of the relation between $q_{m,1}$ and $I_{m,1}$ [12,13]. For $t < t_c$ the trajectory of a cooling experiment is always in the two phase region and the coexisting phases are not in equilibrium. This situation corresponds to the early and intermediate stage of isothermal phase formation. In the early stage of demixing the characteristic structure length Λ is expected to decrease in cooling experiments with the undercooling by $\Lambda \propto \Delta T^{-\nu}$, where ν is critical exponent of the correlation length (Ising model: $\nu = 0.63$). This stage was too short to be detected in our SALS experiments. The late stage of demixing is usually characterized by a thermodynamic equilibrium of the coexisting phases (which are still growing) and a composition of the two phases which is identical to the binodal composition. In the continuous cooling experiment for $t > t_c$ the difference between the compositions of the phases is increasing with further undercooling $\Delta T(t)$ and the characteristic structure length $\Lambda(t)$ is expected to increase by a hydrodynamic coarsening mechanism [1] with $d\Lambda / dt \propto \Delta T^z$ [12, 13]. The exponent z is given by $z = \mu + \nu \cdot x_\eta$, where μ and x_η are the critical exponents of surface tension and viscosity respectively. The mean field value is $z = 1.5$ and the 3D-Ising model yields $z = 1.30$ [14]. A detailed analysis [12, 13] of the $q_{m,1}(\Delta T)$-curves yields $z = 1.68$, which is in the right order of magnitude. The $q_{m,1}$ ($= 2\pi/\Lambda$) vs. ΔT curves in Figures 3 indicate the expected power law behavior for $\Delta T > \Delta T_c$. Following these arguments in late stage of continuous cooling experiments a competition between the mass transfer due to diffusion and the growth of the two phase structure has to be expected. When the growth rate of the characteristic structure length $v_{str} \propto d\Lambda/dt$ becomes equal to or larger than the rate of the mean squared spatial displacement of the molecules ("diffusion velocity")

$v_{diff} \propto d\sqrt{D(t)t}/dt$ (D: mutual diffusion coefficient) the thermodynamic equilibrium of the coexisting phases is not guaranteed and a secondary phase separation inside the domains can occur (see Scheme II). The characteristic undercooling ΔT_s for this secondary phase separation is expected to depend on the cooling rate by $\Delta T_S \propto \kappa^{1/(2z+1-\nu^*)}$ [12, 13], where ν^* is the critical exponent for the diffusion coefficient (Ising model: $\nu^* = 0.63$, mean field theory: $\nu^* = 0.5$). For the reaction-induced phase separation the formation of a secondary structure inside the domains is usually explained by the increase of the viscosity due to gelation or vitrification. However, for PEMS and PDMS the viscosity does not change significantly in the temperature interval of the experiments and both glass transition temperatures are very low. Therefore the secondary phase separation in binary mixtures can be explained by kinetic arguments, without the assumption of a gelation or vitrification.

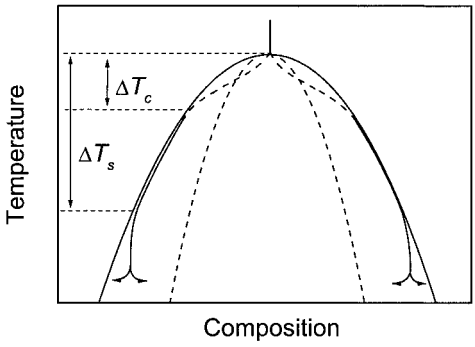

Scheme II. Cooling trajectory in the phase diagram of a binary mixture.

Reaction-Induced Phase Separation

In Figure 5 the time evolution of the scattering intensity during isothermal reaction of an epoxy mixture with 15 wt% PSU cured at 80°C is shown (see ② in Figure 1). Similar to evolution of the scattering intensity in the course of cooling of the PEMS/PDMS blend in Figure 2, two maximum in the scattering intensity become visible after the phase separation. The maximum intensity of the first peak, I_{m1}, increases and the related scattering vector, q_{m1}, decrease with time. The final

morphology (see micrograph in Figure 6) is bicontinuous and the major scattering maximum can be related to reaction-induced spinodal decomposition. The open points q-values are calculated by $q_{m,1} = 2\pi/\Lambda_{OM}$, where the characteristic structure length Λ_{OM} was estimated from time resolved OM. The appearance of a second maximum in the scattering intensity at later times can be related to the secondary phase separation in the epoxy- and the PSU-rich phase. The micrograph in Figure 6 shows secondary structures in both phases. The maximum scattering intensity of the second peak, I_{m2}, is assumed to be an average of the secondary structures inside both phases. As expected I_{m2} increases with reaction time and the related q-value decreases (left graph in Figure 6).

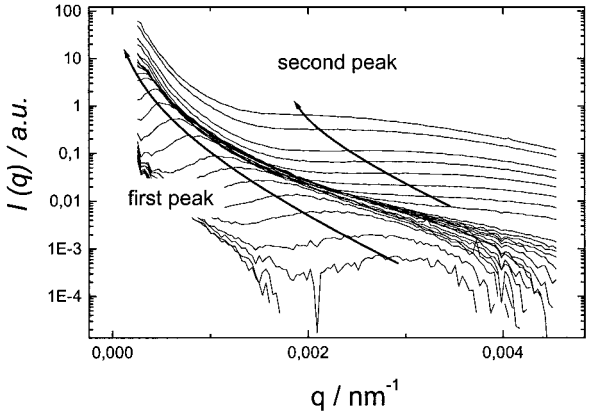

Figure 5. Time evolution of the scattering intensity *I(q)* during isothermal reaction of an epoxy mixture with 15 wt% PSU cured at 80°C.

The main characteristic of the epoxy mixture with 15 wt% PSU is the 'pinning' of the primary phase structure (corresponding to the first peak) as observed with OM occurs at about 17 min after the phase separation (leveling-off of $q_{m,1}$ in Figure 6). A deflection for the evolution of $q_{m,2}$ is also observed at this time. This 'pinning' was attributed to the viscosity increase due to approaching vitrification of PSU-rich phase.

The first appearance of the secondary structure is found to occur considerably before the gelation and vitrification of either phase [11]. It is explained by the competition between mutual diffusion and structure growth as for the polymer blends (see above). The corresponding trajectory for the "critical" thermoset/thermoplastic mixture is shown in a schematic conversion versus

composition diagram (left figure in Scheme III). A secondary phase separation has been found inside both primary phases considerably before the gelation and vitrification of one of the phases.

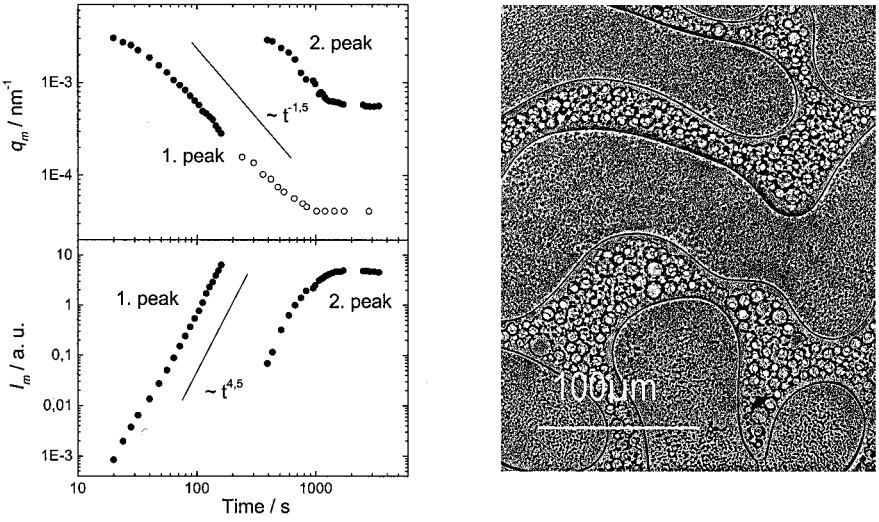

Figure 6. Time evolution of q_m (upper part) and I_m (lower part) for an epoxy / PSU mixture with 15 wt% PSU cured at 80°C. The open symbols are estimated from optical microscopic images. The right picture represents the 'pinned' domain structure 17 minutes after phase separation.

In Figure 7 the time evolution of the scattering vector at maximum intensity (upper part), the maximum scattering intensity (middle part) and the conversion (lower part)) for an epoxy/PSU mixture with 25 wt% PSU cured at 70°C, 80°C and 90°C are shown (see also ③ in Figure 1). As indicated in the electron micrograph in Figure 7 the mixture with 25 wt% PSU forms droplets of the epoxy-rich phase embedded in the PSU-rich matrix. Therefore the scattering maximum has to be related to scattering on droplets with a mean interspherical distance $\Lambda_s = 2\pi / q_{m,s}$. For the evolution of these epoxy-rich droplets a nucleation and growth mechanism can be assumed. The appearance of a maximum in *I(q)* in blends with a nucleation and growth mechanism is well known. It can be caused by coherent scattering of the droplet ensemble or a by depletion zones around the droplets [12,15,16]. Here we assume the first to be dominant because of a high droplet

density. This can also explain higher order scattering peaks. The maximum has also been found for non-critical PEMS/PDMS mixtures and was simulated by the Rayleigh-Gans theory [12].

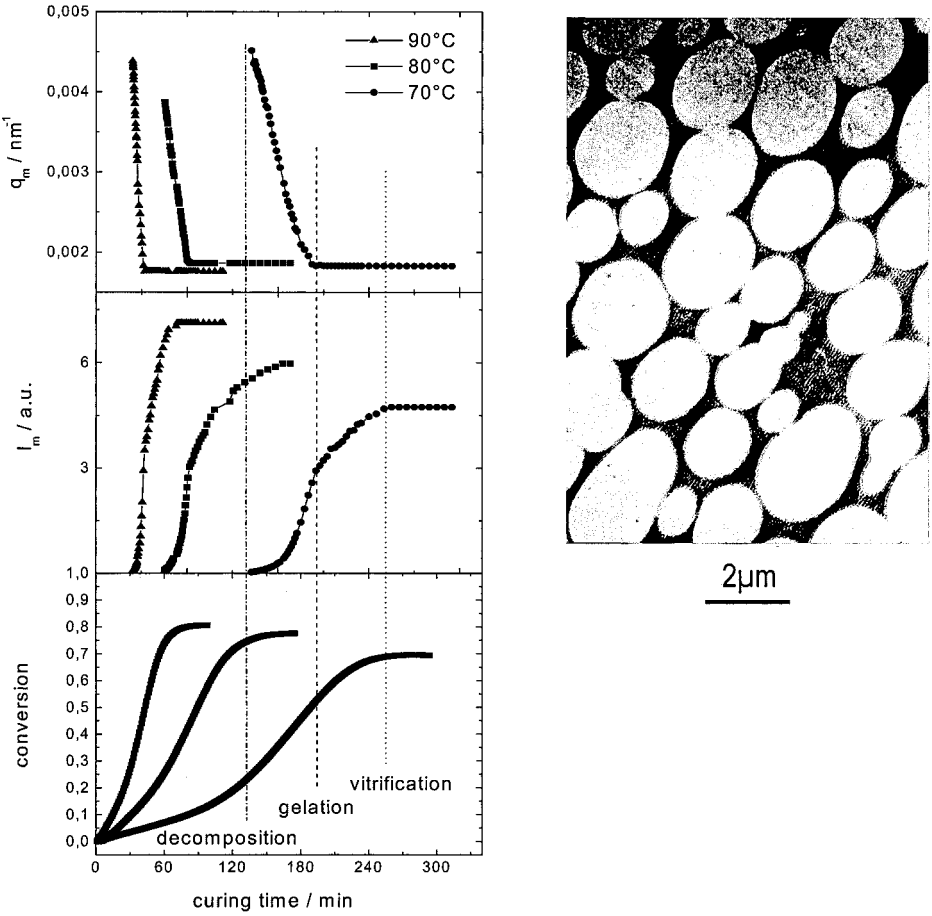

Figure 7. Time evolution of q_m (upper part), I_m (middle part) and conversion (lower part) for an epoxy/PSU mixture with 25 wt% PSU cured at different temperatures. The domain structure after 400 minutes curing at 80°C is shown in a transmission electron micrograph (right part).

It is obvious that the curves of q_m and I_m versus time for the three different curing temperatures have the same shape. The curves can be subdivided into four regions: (i) no scattering signal, (ii) strong decrease of $q_m(t_{cure})$ and strong increase of $I_m(t_{cure})$, (iii) leveling-off of $q_m(t_{cure})$ and lower slope in $I_m(t_{cure})$, and (iv) leveling-off of $I_m(t_{cure})$. The appearance of the maximum of scattered light intensity in the time interval (ii) is an indication for the phase separation. The epoxy reaction is assumed to proceed in both phases. As we have found by temperature-modulated calorimetry (isothermal experiments) the PSU-rich matrix vitrifies ($T_{cure} \cong T_g(t_{cure})$) at the beginning of the interval (iii), which can explain that structure growth stops. However, a considerable amount of reaction in the epoxy-rich phase is still occurring. Finally the reaction stops also in the epoxy-rich droplets by vitrification (interval iv). The characteristics for the "non-critical" thermoset/thermoplastic mixture, shown in the right figure of Scheme III, are the large differences in the conversions of the two phases which are necessary for vitrification, and that no secondary phase separation could be detected.

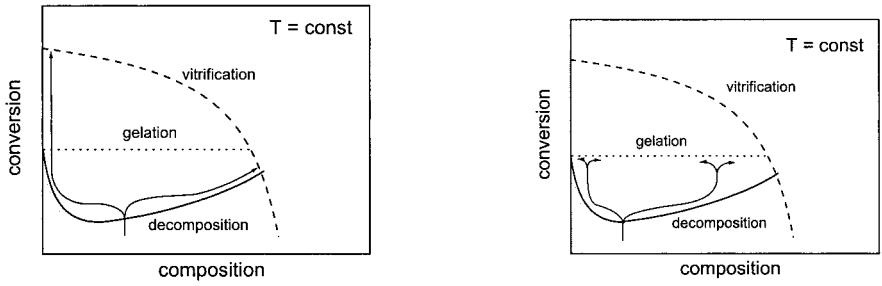

Scheme III. Conversion vs. composition diagrams with reaction trajectories for a "critical" (left) and a "non-critical" thermoset/thermoplastic mixture (right).

Similar to the *cooling rate scaling* for the binary blend one would expect here a *reaction rate scaling*. The similar shapes of the $q_m(t_{cure})$ and $I_m(t_{cure})$ curves for different temperatures in Figure 7 are an indication for that. To construct a master curve for reaction-induced phase separation the reaction time has to be replaced by the conversion and the dependence of the (local) viscosity on the conversion has to be taken into consideration.

Conclusion

Continuous quenches into the two phase region (Scheme I) can be realized by increase of χ (cooling or pressure ramps) or N (polymerization reaction). It has been shown that the continous χ-induced decomposition realized by cooling ramps in polymer mixtures and the N-induced decomposition in a reaction-induced phase separation show similar features in time resolved SALS experiments. For both cooling-induced and reaction-induced phase separation the appearance of a fine structure due to secondary phase separation was detected. It has been shown that secondary (and probably ternary and higher order) phase separation can be explained by the competition between structure growth and mutual diffusion.

Universality of structure growth for different cooling rates, *cooling rate-scaling*, was observed for the binary polymer blend and can be explained by the critical behavior of correlation length, diffusion coefficient, viscosity and surface tension. Similar behavior, *"reaction rate-scaling"*, can be expected for the polymerization-induced phase separation, where the viscosity increase during reaction has to be taken into account.

The financial support from the Bundesministerium für Wirtschaft und Technologie through the AiF (11540N) and the Deutsche Forschungsgemeinschaft (Al 396/3-2) is gratefully acknowledged.

[1] T. Hashimoto, in: *Materials Science and Technology* , E. L. Thomas, Ed., VCH, Weinheim 1993, Vol.12, Ch.6.
[2] H. O. Carmesin, D. W. Heermann, K. Binder, *Z. Phys.* B **1986**, *65*, 89.
[3] S. A. Kukushkin, V. V. Slyozov, *J. Phys. Chem. Solids* **1995**, *56*, 1259.
[4] S. A. Kukushkin, V. V. Slyozov, *J. Phys. Chem. Solids* **1996**, *57*, 195.
[5] S. A. Kukushkin, V. V. Slyozov, *J. Phys. Chem. Solids* **1996**, *57*, 601.
[6] T. Hashimoto, M. Hayashi, H. Jinnai, *J. Chem. Phys.* **2000**, *112*, 6886.
[7] M. Hayashi, H. Jinnai, T. Hashimoto, *J. Chem. Phys.* **2000**, *112*, 6897.
[8] J. P. Pascault, H. Sauterau, J. Verdu, R. J. J. Williams, *Thermosetting Polymers* , Marcel Dekker Inc., New York 2002.
[9] B. Steinhoff, M. Rüllmann, L. Kühne, I. Alig, *J. Chem. Phys.* **1997**, *107*, 5217.
[10] I. Alig, W. Jenninger, J.E.K. Schawe, *Polymer* **2000**, *41*, 1577.
[11] M. Holst, J. Xu, M. Rüllmann, M. Wenzel, I. Alig, *Macromolecules* (in preparation).
[12] M. Rüllmann, *PhD Thesis*, Darmstadt 2002.
[13] M. Rüllmann, I. Alig, *J. Chem .Phys.* (in preparation).
[14] A Stammer, B. A. Wolff, *Polymer* **1998**, *39*, 2065; W. Theobald, G. Meier, *Phys. Rev. E* **1995**, *51*, 5776
[15] G. E. Elicabe, H. A. Larrondo, R. J. J. Williams, *Macromolecules* **1997**, *30*, 6550.
[16] G. E. Elicabe, H. A. Larrondo, R. J. J. Williams, *Macromolecules* **1998**, *31*, 8173.